

Adsorption and Reactivity of CO₂ on Defective Graphene Sheets

Pepa Cabrera-Sanfelix

Donostia International Physics Center (DIPC), Paseo Manuel de Lardizabal 4, San Sebastian 20018, Spain

Received: August 08, 2008; Revised Manuscript Received: October 31, 2008

Density-functional calculations have been performed to investigate the adsorption of CO₂ on defected graphite (0001) represented by a single graphene sheet. The interaction with a vacancy defect gives a computed molecular binding energy of ~ 136 meV in a strong physisorbed state. Subsequently, chemisorption by lactone group formation will occur after overcoming a barrier of ~ 1 eV relative to the gas phase, with an exothermicity of about 1.4 eV. Further reaction paths from this chemisorbed state lead to dissociation of the CO₂ through the formation of epoxy groups followed by oxygen recombination and desorption of O₂, after overcoming successive energy barriers of ~ 0.9 and ~ 1.0 eV. The global minimum (“O₂ desorbed + graphene sheet”) entails an energy release of about 3.4 eV with respect to the initial state.

1. Introduction

The adsorption and reactivity of CO₂, among other gases, on carbonaceous surfaces is a subject of great interest in the technological and atmospheric fields. Gas adsorption in carbon nanotubes (CNTs) and CNT bundles modifies their properties and therefore their possible technical applications.^{1–5} For example, it has been demonstrated that the electrical resistance of a semiconducting single-walled carbon nanotube (SWNT) changes dramatically upon exposure to gaseous molecules such as NO₂ or NH₃.⁶ In field emission applications, the influence of various residual gases in the vacuum chamber is a critical factor for the long-term stability of CNTs.^{7–9}

From the atmospheric point of view, the reduction of the CO₂ concentration on the atmosphere is an urgent requirement. Industrialization has raised the atmospheric CO₂ concentration from 280 to 370 ppm (ppm), which seems to be the primary cause of the average global surface temperature rise of 0.6 °C over the past century.¹⁰ Sequestration of the greenhouse gas CO₂ is therefore one of the most pressing issues in environmental protection. This makes the study of the interaction of CO₂ with several substrates a subject of great interest.

The adsorption of CO₂ on graphitic surfaces has been experimentally and theoretically investigated in the past few years.^{11–21} Jiang and Sandler used C₁₆₈ schwarzite for separation and capture of CO₂ among other pollutant gases.²¹ The curved surface of C₁₆₈ schwarzite, due to the combination of the aromatic sp² and aliphatic sp³ carbon atoms, provides a more attractive gas–carbon interaction potential than that for planar graphite, which uniquely contains sp² carbon atoms forming the aromatic rings. The gas–carbon interaction potential is therefore influenced by the surface curvature and ring structure, which changes the localization of the electron density. The curvature-induced charge redistribution and polarization has also been studied for CNTs.²² Neutron diffraction experiments by Bienfait et al.¹³ showed the adsorption of CO₂, and other gas molecules, on the grooves sites of SWNTs bundles. Yim and co-workers¹⁶ combined infrared spectra with local density approximation density functional theory (DFT-LDA) to investigate CO₂ adsorption at different graphitic surfaces. They found preferred adsorption of CO₂ on the grooves and interstitial sites of bundles of SWNTs. Weaker CO₂ binding was found on a single SWNT in which the molecule showed preferential adsorption on the

internal surface of the nanotube. The lowest binding energy was reported for the CO₂ adsorption on the graphene layer, ~ 147 meV. A similar DFT-LDA investigation by Zhao et al.¹⁸ showed physisorption of CO₂ on the graphene layer with a comparable binding energy, ~ 151 meV. However, both DFT values for the adsorption energy are slightly lower than the experimental values, 178 meV.²³ Montoya and co-workers also combined experiment and theory (B3LYP-DFT) to provide further insight into the mechanism of CO₂ chemisorption on graphene sheets.²⁰ Their experiments found a variation in the adsorption energy, from ~ 3.7 eV to ~ 200 meV, suggesting a broad spectrum of active binding sites, such as edge sites, pre-adsorbed alkali metals, and defects. The most stable complex formed by the chemisorption of CO₂ on the graphene edge sites was the lactone group on the armchair edge, with an adsorption energy of 3.68 eV. As the CO₂ coverage increases, the adsorption energy drops to hundreds of meV. This was attributed to the fact that active sites were already occupied, so further CO₂ molecules could only physisorb on the graphene planes. Xu et al.¹⁷ investigated the possible dissociative adsorption of CO_x on free-defect graphite (0001) surface. The reported reaction products were oxidized graphite (epoxy groups) and a chemisorbed lactone group. However, all the reactions were found to be highly endothermic and the reaction pathways were associated with considerable forward energy barriers, possible to overcome only under high-temperature and high-pressure conditions. On the other hand, high temperature will rather lead to rapid desorption of the adsorbate molecule instead of aiding any chemical reaction. Therefore, any dissociative reaction process has to be accompanied by a directional force pushing the adsorbate molecule to the surface. Allouche and Ferro¹⁹ studied the possible adsorption of CO₂ among other small molecules at single vacancies on a defected graphite (0001) surface. They found that some of the molecules, such as H₂, O₂, and H₂O, chemisorbed dissociatively on the vacancy defect, whereas for the CO₂ molecule they reported only a local minimum of ~ 200 meV, corresponding to the physisorption state.

Contrary to the results of Allouche and Ferro, our DFT-GGA calculations clearly indicate that CO₂ chemisorption occurs exothermically on the single vacancy defect on the graphite (0001) surface, after overcoming a specific energy barrier. From this chemisorbed state, we have investigated further reaction

products, such as epoxy groups adsorbed on a renewed graphene sheet and a desorbed O₂ molecule by the recombination of the chemisorbed atomic oxygens.

2. Computational Details

All calculations were performed using the Vienna ab initio simulation package (VASP),^{24–26} implementing the density functional theory (DFT) within the Perdew–Wang 1991 (PW91) version of the general gradient approximation (GGA).²⁷ The projector augmented wave (PAW) potentials^{28,29} were used to describe the interaction of valence electrons with the core of the C and O atoms.

The graphite substrate was represented by a single layer using a supercell with periodic boundary conditions along the three spatial directions. One layer of the graphite (0001) basal surface, as confirmed in previous work,³⁰ is sufficient since the interlayer spacing of graphite (≈ 3.4 Å) excludes any strong influence from contiguous layers. To avoid interaction between periodic images along the surface, we have employed a 4×4 supercell. Furthermore, a vacuum gap of 15.7 Å between periodic images of the substrate was checked to be large enough for all calculations. We have used a $3 \times 3 \times 1$ Monkhorst-Pack *k*-point sampling and a plane-wave cutoff of 400 eV in all the calculations, which have been shown to be sufficiently accurate.³¹ Spin polarization was included in all calculations. Most of the atoms of the system were allowed to fully relax until the residual forces were less than 0.03 eV/Å. Only those surface carbon atoms at the largest distance from the vacancy site were fixed to minimize elastic interactions between periodic vacancy defects.

The values for the adsorption energies, E_{ads} , are calculated from

$$E_{\text{ads}} = E_{\text{Graphene}} + E_{\text{CO}_2} - E_{\text{CO}_2/\text{Graphene}} \quad (1)$$

where E_{Graphene} and E_{CO_2} correspond to total energies of the relaxed defected surface and of the isolated CO₂ molecule, respectively. $E_{\text{CO}_2/\text{Graphene}}$ is the energy of the optimized system. The chemisorption pathway of CO₂ has been determined by approaching the molecule in steps of 0.2 Å and optimizing the geometry at each molecular height so only the *z*-coordinate of the molecule C atom remains fixed. In the following, molecular heights refer to the difference between the *z*-coordinate of the central carbon atom of CO₂ and that of one of the fixed carbon atoms on the graphite (0001) basal plane.

Further reaction paths starting from the chemisorbed state have been determined by bringing the molecular C toward the vacancy site, so the “C–vacancy” distance is kept fixed at each step. This leads to a first transition state in which the molecule dissociates with the C atom filling the vacancy and the O atoms chemisorbed as epoxy groups. From this state, we have proposed a second path by drawing the oxygen atoms toward each other, keeping the “O–O” distance fixed at each relaxation step.

Vibrational frequencies for the physisorbed CO₂, for the chemisorbed lactone group, and for the chemisorbed epoxy complexes have been computed by fixing the main part of the C atoms on the graphene layer. Therefore, we have considered only the 12 C atoms surrounding the vacancy defect and the C and O atoms of the CO₂. We have also calculated the vibrational modes of the CO₂ in the gas phase to compare with the different configurations found in this work.

3. Results

It is accepted that the perfect (0001) basal plane of graphite represents a good surface science model to reproduce molecular

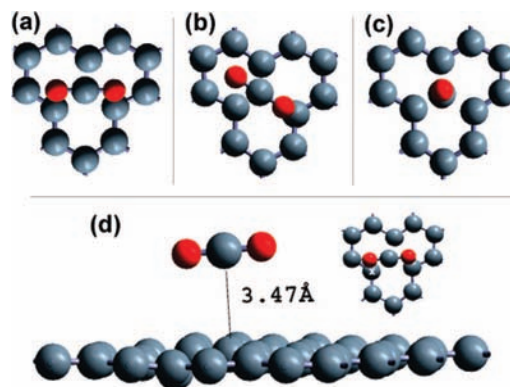


Figure 1. (a), (b) and (c) panels correspond to the three initial configurations proposed for the physisorption of CO₂ on the defected (0001) graphene sheet. The optimized physisorbed state is represented in panel (d). This structure is obtained from both (a) and (b) initial guesses.

adsorption and interaction with carbonaceous particles. However, the clean perfect surface is only a first-order model and its reactivity is very low.^{16,18,30} Vacancies are common defects in crystalline solids and affect their physical properties. Very low concentrations of vacancy defects occur in graphite³² during growth and at thermal equilibrium at ambient conditions. These defects are much more prevalent in electron or ion irradiated materials and are believed to be the predominant defects on irradiated graphitic surfaces.³³ Various experimental techniques have been used to investigate the structure and properties of vacancies in graphite and CNTs.^{33–36} Recent tight-binding molecular dynamic simulations determined that the recombination of single-vacancy defects in the graphene layer involves a large energy barrier that entails heating the graphite surface to 3000 K.^{37,38} Therefore, mending of single vacancies is not expected at ambient temperature.

In previous DFT calculations, we have determined that water molecules can dissociatively chemisorb at the vacancy defects of the (0001) basal plane of graphite, after overcoming a moderate energy barrier. In the highly exothermic chemisorbed state, the triatomic molecule dissociates completely, forming new C–H, and C–O covalent bonds with the C atoms surrounding the vacancy.³¹ In this work, we are interested in the possible interaction of a different triatomic molecule, CO₂, with the same type of defect. Although DFT cannot account for van der Waals type binding, and we cannot place any significance on the physisorption well depth or corrugation, we have investigated the possible physisorption by placing the CO₂ at three different orientations above the graphite surface, with the central carbon atom on top of the vacancy defect (see Figure 1). In the first configuration (Figure 1a) the molecule has an initial height of 2.5 Å and keeps its molecular axes parallel to the graphite surface. In the second configuration (Figure 1b) the molecule is still parallel to the surface but rotated 30° with respect to the structure in Figure 1a. In the third configuration (Figure 1c) the molecule is perpendicularly oriented to the surface, with the lower oxygen atom placed 2.5 Å above the vacancy, so the central C atom seats 3.67 Å above the surface. During relaxation, configurations of Figure 1a,b relax to the same optimum state (Figure 1d) in which the parallel molecule rises to ~ 3.47 Å above the surface, with both O atoms almost on top of two C atoms around the vacancy and with a physisorption energy of ~ 136 meV. On the other hand, the initially perpendicular molecule in Figure 1c tilts $\sim 60^\circ$ around its central C atom and moves up to 3.96 Å above the surface, as a consequence of the repulsion between the electrons in the

TABLE 1: Calculated Vibrational Frequencies (cm⁻¹) for the Different Adsorption Geometries of CO₂ on Defected Graphene

	phys. CO ₂ on def. graphene	chem. CO ₂ lactone complex	chem. CO ₂ epoxy complexes
C=O stretching	2356 ^{Antisym.} 1322 ^{Sym.}	1758	
C–O stretching		1357 1099	837
C–C stretching ^a			872 1443 ^{Sym.} 1416 ^{Antisym.}
C=O stretching ^b	2352 ^{Antisym._gas_phase} 1285 ^{Sym._gas_phase}		

^a Refers to the C–C bond forming the epoxy group. ^b Computed stretching of gas-phase CO₂.

unsaturated bonds of the carbon atoms in the vacancy and the lower oxygen atom of the CO₂ molecule. Thus, the molecule stays less bounded to the surface, $E_{\text{ads}} = 117.4$ meV, compared to the optimum physisorbed state. The optimum physisorption energy obtained here using GGA-PW91, ~ 136 meV, is slightly lower than the DFT-LDA values given for CO₂ adsorption on perfect graphene, ~ 147 – 151 meV.^{16,18} Although one expects a lower binding energy of CO₂ on a perfect graphene sheet, LDA tends to exaggerate the covalent component, partially compensating the lack of dispersive interactions in DFT, and therefore, it overestimates the adsorption of the molecule.

Although the physisorption energy found in this work indicates low reactivity of the vacancy defect with the CO₂ molecule, still this rather weak interaction induces one of the C atoms at the surface to move ~ 0.4 Å down from the graphite plane (x-marked C atom on the inset of Figure 1d). The vibrational frequency of the asymmetric stretching for CO₂ physisorbed on the defected graphene surface was calculated to be 2356 cm⁻¹. This value is comparable to the computed asymmetric mode for CO₂ in the gas phase, 2352 cm⁻¹ (see Table 1). The calculated C=O symmetric stretching mode for the physisorbed CO₂ on defected graphene, 1322 cm⁻¹, shifts by 37 cm⁻¹ with respect to the computed symmetric stretching of CO₂ in the gas phase, 1285 cm⁻¹. The calculated frequencies for CO₂ physisorbed on the defected graphene compared with the ones reported by Yim and co-workers for CO₂ adsorbed on a perfect graphene layer.¹⁶

It has been previously shown that defected graphite is substantially more reactive than a perfect graphite plane for small molecules, which dissociate at the vacancy after overcoming moderate energy barriers.^{17,31,39} In this work, we have investigated the interaction of CO₂ by first placing the molecule very close from the surface and perpendicularly oriented to the graphite plane, as in Figure 1c. So the downward oxygen atom is at the same height of the graphene plane. During relaxation the molecule dissociates into CO and O fractions that remain chemisorbed at the vacancy site, forming new covalent bonds of 1.53 and 1.42 Å, respectively (see Figure 2a). Formation of new bonds makes this optimized state highly exothermic, ~ 2.41 eV, with respect to CO₂ in the gas phase. To estimate the required energy barrier to obtain this dissociated configuration, we have constrained the x , y , and z coordinates of each molecular

atom, so CO₂ moves perpendicularly toward the surface. This highly unfavorable approaching orientation results in a very large energy barrier, ~ 5.3 eV, making this chemisorption state unlikely in spite of the high exothermicity (see Figure 2c). In a different approach, we have allowed full relaxation of the perpendicular CO₂ molecule when it is close to the surface but still slightly separated from the graphene plane. In this case, the CO₂ molecule desorbs from the surface in a dissociated manner, leaving one oxygen atom chemisorbed in the vacancy, as illustrated in Figure 2b. This state leads to an energy released of ~ 1.52 eV. The required energy barrier in this case also has to be estimated by the approach of perpendicularly oriented CO₂ toward the surface. However, in an attempt at reducing the energetic cost of the perpendicular approach, we have allowed stretching of the CO₂ inner axes. Thus, uniquely the downward oxygen and the x and y coordinates of the two other molecular atoms were fixed at each approaching step. With these constraints the energy barrier was still very high, ~ 3.3 eV. As expected, relaxation of the inner bonds leads to different reaction products since the CO desorbs from the surface whereas the remaining O atom replaces the missing carbon in the defected graphene sheet, as illustrated in Figure 2b. Both types of dissociative chemisorption are very exothermic, -2.41 and -1.52 eV; however, the approaching paths have to be accompanied by a directional force at all heights to maintain the molecule perpendicular to the surface; otherwise, the molecule would rotate until it was quasi-parallel to the surface. This constraint accounts for the extremely high energy barriers in both cases. Therefore, we assume that neither of the chemisorption states presented so far is likely to be populated.

A more reasonable chemisorption path is found by approaching the molecule freely toward the substrate. So, at each step of the pathway ($\Delta Z = -0.2$ Å), we have uniquely fixed the height of the molecule C atom. Consequently, the molecule orients its inner axis, keeping it parallel to the surface during the whole path. After overcoming an energy barrier of ~ 1 eV the system converges into an equilibrium state in which the molecule chemisorbs, forming a lactone group as shown in Figure 3 a. This configuration is similar to the one found by Montoya and co-workers²⁰ for CO₂ adsorption on graphene armchair edges. In our case, the central C and one O atom of the CO₂ molecule are directly bonded to the C atoms around the vacancy, forming bond lengths of 1.74 and 1.96 Å, respectively. The molecule is bent with an internal angle of 153.4°, so the remaining C=O bond is pointing up from the surface. Despite the lower exothermicity of this configuration, ~ 1.43 eV, compared with the previous dissociative chemisorption states, this last configuration is more likely to occur as the energy barrier has decreased to ~ 1 eV (see Figure 3b). Therefore, we believe that chemisorption of CO₂ can occur at a vacancy defect on graphite by forming a “lactone complex”, with an energy released of ~ 1.43 eV. Notice the disruption around the vacancy as a consequence of the emergence, by about ~ 0.2 and ~ 0.6 Å, of the C atoms bonded respectively to the C and O atoms from the molecule.

We have also calculated the vibrational modes for this stable lactone configuration. The most intense frequency value, 1758 cm⁻¹, corresponds to the C=O stretching mode, whereas further modes are found at 1357 and 1099 cm⁻¹ for the stretching of C–O bonds (see Table 1). These vibrational modes are comparable to the infrared vibrational frequencies of the lactone complex formed by CO₂ adsorption on the armchair edges of the graphene layer, predicted by Montoya and co-workers.²⁰

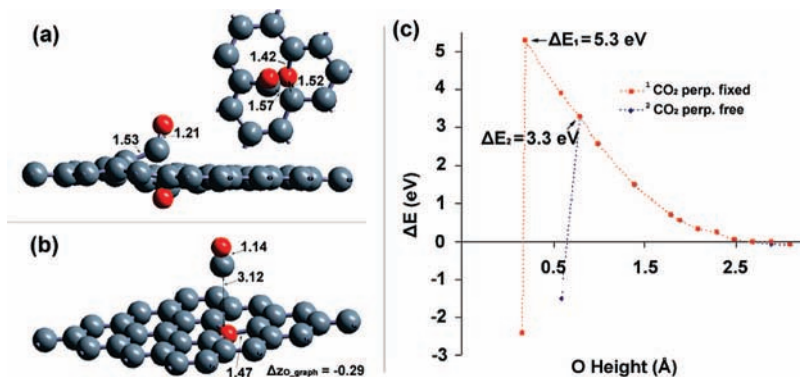


Figure 2. (a) Illustration of the dissociative CO₂ chemisorption at the vacancy defect. (b) The oxygen incorporated into vacancy and the desorption of the remaining CO. Both configurations come from the perpendicular approach of the CO₂ molecule toward the surface. Notice that, in all figures, the numerical values are given in Å. (c) Energy curves as a function of the height of the oxygen atom from the CO₂ molecule that points toward the surface.

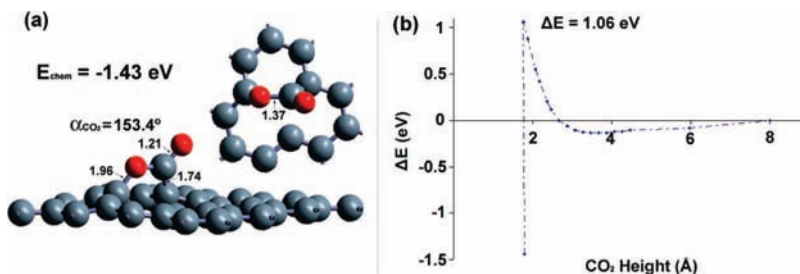


Figure 3. (a) Chemisorption of CO₂ as a lactone complex on the vacancy defect of the graphene layer. (b) Energy curve as a function of the height of the molecular C atom for the CO₂ approaching path from the gas phase.

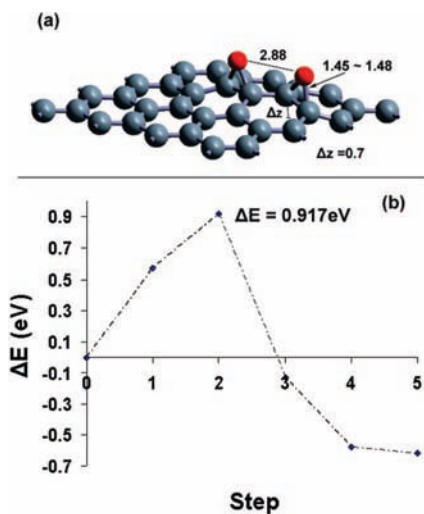


Figure 4. (a) CO₂ chemisorption as epoxy complexes on the graphene surface. (b) Energy curve as a function of the approaching steps of the C atom from the lactone complex toward the vacancy.

Further reaction products from the lactone chemisorbed state have been proposed and their feasibility has been investigated through the calculation of reaction pathways. The configuration of Figure 4a corresponds to the final state found by pushing the C atom from the lactone group toward the vacancy gap in small steps of 0.2 Å. We have fixed the position of this particular carbon and relaxed the rest of the system at each approaching step. This path has an energy barrier of ~ 917 meV (see Figure 4b) with respect to the previous stable lactone complex, shown in Figure 3a. At this new minimum configuration (Figure 4a) the oxygen atoms from the decomposed molecule remain chemisorbed on the surface forming epoxy groups, C–O–C bond lengths of ~ 1.45 – 1.48 Å, inducing a surface buckling of ~ 0.7 Å at the highest protrusion. The C atom from the

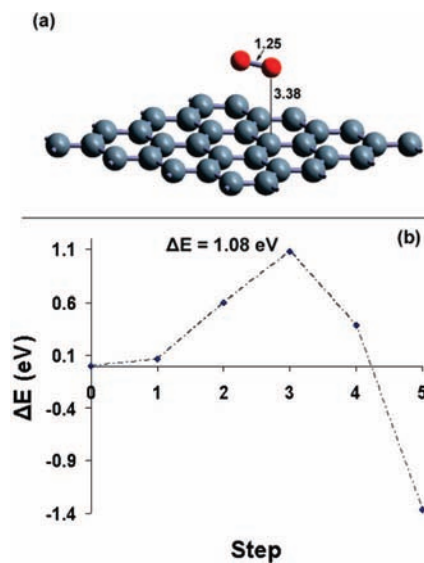


Figure 5. (a) Optimized O₂ desorption from the restructured graphene sheet. (b) Energy curve as a function of the oxygen–oxygen approaching steps, starting from the epoxy-complexes configuration (Figure 4a).

decomposed CO₂ fills the vacancy defect, restoring the complete graphene sheet. This arrangement is ~ 614 meV more stable than that of the lactone complex.

In this case, the stretching of the C–C atoms forming the epoxy groups occurs symmetrically at 1443 cm⁻¹ and antisymmetrically at 1416 cm⁻¹. We observe the stretching of the C–O bonds at frequencies of 837 and 872 cm⁻¹ (see Table 1).

We consider the epoxy-complexes configuration as the initial state for further reaction presented in Figure 5a, which consists of a O₂ molecule desorbed from the restored graphene sheet as a consequence of the recombination of the O atoms forming

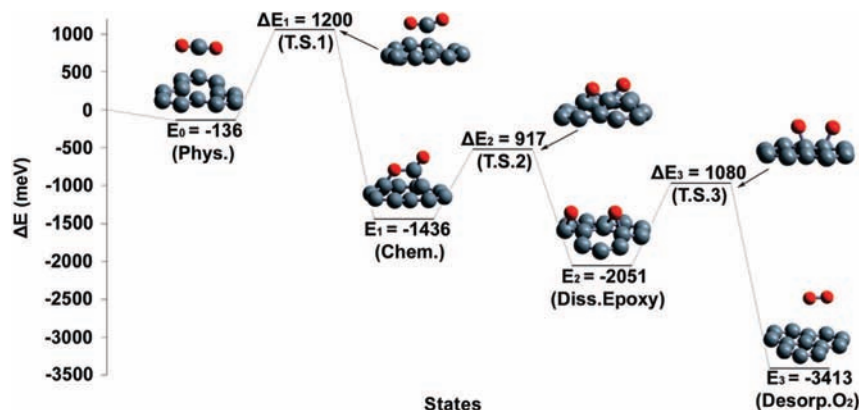


Figure 6. Main structural and energetic scheme of the proposed global reaction path for the interaction of CO₂ with the defective graphene layer. The given energies at the local minimum are relative to gas phase. The energy barriers at the transition states (T.S.) are relative to the immediate preceding chemisorbed (chem.) and physisorbed (phys.) state.

the epoxy groups. The O₂ desorption leads to an energy release of ~ 1.36 eV with respect to the epoxy-complexes configuration and of ~ 3.4 eV with respect to the gas-phase CO₂. The energy barrier of ~ 1.08 eV (see Figure 5b), has been calculated starting from the epoxy-complexes configuration (see Figure 4a) by approaching the chemisorbed oxygen atoms to each other in small steps of 0.2 Å. At each relaxation step only the x and y coordinates of the O atoms have been fixed, to keep the oxygen–oxygen distance, allowing their detachment from the surface.

Finally, Figure 6 reports all the configurations investigated in this work through the scheme of the global path starting from the system “CO₂ in gas phase + defected graphene sheet” until the final state “desorbed O₂ + perfect graphene sheet”. The different local minimum configurations and the transition states at the energy barriers are also included. Notice that the released energy at the local minimum states is referred to the gas phase, whereas the energy barriers are relative to the preceding stable configuration. From the energetic point of view, one could think of this global process as a possibility for carbon capture and could be thought as a simple model for the fixing of gaseous CO₂ molecules at defective carbon structures.

4. Conclusions

In this work we performed density-functional calculations to investigate the adsorption and reactivity of CO₂ on a defected graphene sheet. Physisorption of the molecule occurs on the top of the vacancy defect, with the inner axis of the molecule parallel to the surface. The computed binding energy of ~ 136 meV indicates a strong physisorption state. From this physisorption state, the chemisorption of CO₂ occurs by forming a lactone group with the C atoms surrounding the vacancy. This configuration takes place after overcoming an energy barrier of ~ 1 eV and it involves an energy release of about 1.4 eV. Further reaction paths from the lactone chemisorbed state show dissociation of the CO₂ through the formation of epoxy groups, which is more stable than the preceding lactone group by ~ 614 meV. Next, we considered the oxygen recombination from the epoxy groups and the desorption of O₂ as the global minimum, with an energy release of ~ 3.4 eV with respect to the gas phase and with an energy barrier of ~ 1.08 eV relative to the previous epoxy-complexes configuration. Energetically, the global pathway has been shown feasible, and therefore, it provides a plausible mechanism to fix and remove gaseous CO₂ molecules. This could motivate further work oriented toward the same atmospheric problem on other defects in graphite and graphene.

Acknowledgment. We acknowledge support from Basque Departamento de Educación, UPV/EHU (Grant No. IT-366-07), the Spanish Ministerio de Educación y Ciencia (Grant No. FIS2007-66711-C02-02), and ETORTEK research contracts “Nanomateriales” and “Nanotron” funded by the Basque Departamento de Industria and the Diputación Foral de Guipuzcoa. Grateful acknowledgments also go to Dr. Daniel Sanchez-Portal, Prof. Andres Arnau, and Dr. George Darling for their comments.

References and Notes

- (1) Dai, H. J.; Hafner, J. H.; Rinzler, A. G.; Colbert, D. T.; Smalley, R. E. *Nature* **1996**, *384*, 147.
- (2) Wong, S. S.; Joselevich, E.; Woolley, A. T.; Cheung, C. L.; Lieber, C. M. *Nature* **1998**, *394*, 52.
- (3) Deheer, W. A.; Chatelain, A.; Ugarte, D. *Science* **1995**, *270*, 1179.
- (4) Baughman, R. H.; Cui, C. X.; Zakhidov, A. A.; Iqbal, Z.; Barisci, J. N.; Spinks, G. M.; Wallace, G. G.; Mazzoldi, A.; De Rossi, D.; Rinzler, A. G.; Jaschinski, O.; Roth, S.; Kertesz, M. *Science* **1999**, *284*, 1340.
- (5) Tans, S. J.; Verschueren, A. R. M.; Dekker, C. *Nature* **1998**, *393*, 49.
- (6) Kong, J.; Franklin, N. R.; Zhou, C. W.; Chapline, M. G.; Peng, S.; Cho, K. J.; Dai, H. J. *Science* **2000**, *287*, 622.
- (7) Dean, K. A.; Chalamala, B. R. *Appl. Phys. Lett.* **1999**, *75*, 3017.
- (8) Wadhawan, A.; Stallcup, R. E.; Perez, J. M. *Appl. Phys. Lett.* **2001**, *78*, 108.
- (9) Wadhawan, A.; Stallcup, R. E.; Stephens, K. F.; Perez, J. M.; Akwani, I. A. *Appl. Phys. Lett.* **2001**, *79*, 1867.
- (10) Service, R. F. *Science* **2004**, *305*, 962.
- (11) Chen, L.; Johnson, J. K. *Phys. Rev. Lett.* **2005**, *94*.
- (12) Matraga, C.; Chen, L.; Bockrath, B.; Johnson, J. K. *Phys. Rev. B* **2004**, *70*.
- (13) Bienfait, M.; Zeppenfeld, P.; Dupont-Pavlovsky, N.; Muris, M.; Johnson, M. R.; Wilson, T.; DePies, M.; Vilches, O. E. *Phys. Rev. B* **2004**, *70*.
- (14) Matraga, C.; Chen, L.; Smith, M.; Bittner, E.; Johnson, J. K.; Bockrath, B. *J. Phys. Chem. B* **2003**, *107*, 12930.
- (15) Rivera, J. L.; McCabe, C.; Cummings, P. T. *Nano Lett.* **2002**, *2*, 1427.
- (16) Yim, W. L.; Byl, O.; Yates, J. T.; Johnson, J. K. *J. Chem. Phys.* **2004**, *120*, 5377.
- (17) Xu, S. C.; Irle, S.; Musaev, D. G.; Lin, M. C. *J. Phys. Chem. B* **2006**, *110*, 21135.
- (18) Zhao, J. J.; Buldum, A.; Han, J.; Lu, J. P. *Nanotechnology* **2002**, *13*, 195.
- (19) Allouche, A.; Ferro, Y. *Carbon* **2006**, *44*, 3320.
- (20) Montoya, A.; Mondragon, F.; Truong, T. N. *Carbon* **2003**, *41*, 29.
- (21) Jiang, J. W.; Sandler, S. I. *J. Am. Chem. Soc.* **2005**, *127*, 11989.
- (22) Dumitrica, T.; Landis, C. M.; Yakobson, B. I. *Chem. Phys. Lett.* **2002**, *360*, 182.
- (23) Vidali, G.; Ihm, G.; Kim, H. Y.; Cole, M. W. *Surf. Sci. Rep.* **1991**, *12*, 133.
- (24) Kresse, G.; Hafner, J. *Phys. Rev. B* **1993**, *47*, 558.
- (25) Kresse, G.; Hafner, J. *Phys. Rev. B* **1994**, *49*, 14251.
- (26) Kresse, G.; Furthmüller, J. *Phys. Rev. B* **1996**, *54*, 11169.
- (27) Perdew, J. P.; Chevary, J. A.; Vosko, S. H.; Jackson, K. A.; Pederson, M. R.; Singh, D. J.; Fiolhais, C. *Phys. Rev. B* **1992**, *46*, 6671.

- (28) Blochl, P. E. *Phys. Rev. B* **1994**, *50*, 17953.
- (29) Kresse, G.; Joubert, D. *Phys. Rev. B* **1999**, *59*, 1758.
- (30) Sanfeliix, P. C.; Holloway, S.; Kolasinski, K. W.; Darling, G. R. *Surf. Sci.* **2003**, *532*, 166.
- (31) Cabrera-Sanfeliix, P.; Darling, G. R. *J. Phys. Chem. C* **2007**, *111*, 18258.
- (32) Kushmerick, J. G.; Kelly, K. F.; Rust, H. P.; Halas, N. J.; Weiss, P. S. *J. Phys. Chem. B* **1999**, *103*, 1619.
- (33) Hahn, J. R.; Kang, H. *Phys. Rev. B* **1999**, *60*, 6007.
- (34) Tang, Z.; Hasegawa, M.; Shimamura, T.; Nagai, Y.; Chiba, T.; Kawazoe, Y.; Takenaka, M.; Kuramoto, E.; Iwata, T. *Phys. Rev. Lett.* **1999**, *82*, 2532.
- (35) Thrower, P. A.; Reynolds, W. N. *J. Nucl. Mater.* **1963**, *8*, 221.
- (36) Thrower, P. A. *Br. J. Appl. Phys.* **1964**, *15*, 1153.
- (37) Lee, G. D.; Wang, C. Z.; Yoon, E.; Hwang, N. M.; Ho, K. M. *Phys. Rev. B* **2006**, *74*.
- (38) Lee, G. D.; Wang, C. Z.; Yoon, E.; Hwang, N. M.; Kim, D. Y.; Ho, K. M. *Phys. Rev. Lett.* **2005**, *95*.
- (39) Ammann, M.; Kalberer, M.; Jost, D. T.; Tobler, L.; Rossler, E.; Pigué, D.; Gaggeler, H. W.; Baltensperger, U. *Nature* **1998**, *395*, 157.

JP807087Y